Hindawi
Advances in Polymer Technology
Volume 2023, Article ID 2020247, 15 pages
https://doi.org/10.1155/2023/2020247

Review Article

Measurement Techniques and Methods for the Pressure Coefficient of Viscosity of Polymer Melts

Yang Liao,[1] **Yeyuan Hu**,[1] **Yunxiang Tan**,[1] **Kosuke Ikeda**,[2] **Ryoji Okabe**,[2] **Ruifen Wu**,[2] **Ryota Ozaki**,[2] **and Qingyan Xu**[1]

[1]*Key Laboratory for Advanced Materials Processing Technology, Ministry of Education, School of Materials Science and Engineering, Tsinghua University, Beijing 100084, China*
[2]*Composite Laboratory Research & Innovation Center Mitsubishi Heavy Industries Ltd., Nagasaki 8510392, Japan*

Correspondence should be addressed to Qingyan Xu; scjxqy@mail.tsinghua.edu.cn

Received 18 July 2023; Revised 20 November 2023; Accepted 1 December 2023; Published 18 December 2023

Academic Editor: Rafael Munoz-Espi

Viscosity is a prominent rheological property of polymer, which is affected by temperature, pressure, shear rate, molecular structure, and other factors. Despite the importance of the pressure effect, there remains a paucity of investigations on the dependence of pressure on viscosity compared with other factors, such as shear rate and temperature. Previous research has established that the correlation between pressure and viscosity is usually expressed by the pressure coefficient. In this paper, different measurement techniques and methods for the pressure coefficient of viscosity of polymer melts are reviewed and evaluated on the basis of published experimental data. The capillary rheometer with a pressurized exit chamber is widely employed because of its accuracy and simple use. Besides, the accuracy and relationship of pressure coefficients determined by different methods are discussed.

1. Introduction

Extreme processing conditions such as high pressure, high temperature, and high deformation rate often occur during polymer processing, such as injection molding, film blowing, and extrusion [1]. These processing conditions have an important influence on polymer viscosity. A great deal of previous researches studying viscosity has focused on temperature [2–4] and shear rate [5–7], while the investigations on the effect of pressure on viscosity are still quite scarce. This may be attributed to the inherent difficulties in high-pressure rheological measurements and the instable measurement results by different measurement methods. However, the pressure dependence of viscosity is of great importance in polymer processing, particularly in the selection of injection molding pressure [8–10]. As early as 1957, Maxwell and Jung [11] found that the viscosity of polymer could increase by one or two orders of magnitude when pressure increased from atmospheric pressure to more than 100 MPa. Westover [12] proved that the apparent viscosity of polyethylene increased 10-fold, and the viscosity of polystyrene increased over 100-fold when the hydrostatic pressure changed from 14 to 172 MPa. Therefore, the pressure dependence of melt viscosity cannot be ignored at high pressures.

Usually, the viscosity varies exponentially with pressure. The pressure coefficient β determined by the Barus equation can be used to express the pressure dependence of viscosity [13] as follows:

$$\eta_p = \eta_{p0}\exp(\beta p), \tag{1}$$

where η_p is the viscosity at pressure p, η_{p0} is the viscosity at atmospheric pressure, and p is the hydrostatic pressure of melt.

Values of pressure coefficients for various polymers have been reported, which are typically estimated to be of the order of 10^{-9}–10^{-8} Pa^{-1} [14, 15]. The specific pressure coefficient values of PE, PP, PS PMMA, PαMASN, PC, and ABS are shown in Table 1. The molecular structures of these

Table 1: Pressure coefficients of different polymers.

Materials	Pressure coefficient (GPa^{-1})	Temperature (°C)	Reference
LDPE	16.5 ± 0.5	170–230	[14]
	17.6	200	[10]
	11.0	150	[18]
	18.4 ± 1.8	150–190	[19]
	10	210	[16]
LLDPE	11.7 ± 0.5	150–190	[19]
	14.4	190	[15]
	14	200	[20]
HDPE	10 ± 0.5	150–200	[14]
	10.3 ± 0.3	170–210	[19]
PP	20.5	220	[10]
	22 ± 0.5	190–230	[14]
	21 ± 4.1	190–230	[19]
PMMA	24.5 ± 0.5	220–240	[14]
	44.8 ± 6.6	230–250	[19]
	37	210	[16]
PC	26.6	290	[10]
	31.5 ± 2.1	280–300	[19]
PS	35.5	200	[10]
	41 ± 13.8	162–242	[21]
	43.5 ± 12.1	190–230	[19]
	29 ± 1.5	180–230	[14]
PαMSAN	38.6 ± 12.2	210	[22]
	36.7	210	[16]
ABS	33.7	230	[10]
	31.5	190	[21]
	29	190	[23]

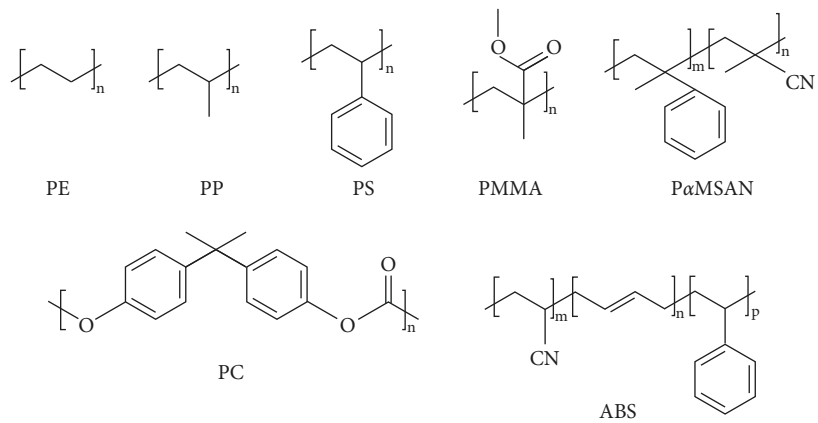

Figure 1: Molecular structures of PE, PP, PS PMMA, PαMASN, PC, and ABS.

polymers are displayed in Figure 1. Obviously, pressure coefficients of polymers with bulkier backbones, like PS or PαMMSAN, are always larger than those of polymers with simple structures, such as PE or PP. It is well known that side groups or bulky backbone groups will stiffen the polymer chain and reduce its flexibility, resulting in a large free volume between molecular chains [10, 15]. When pressure increases, the amount of free volume available between polymer chains decreases. The less the free volume, the stronger the intermolecular interaction [16, 17]. As a result, a corresponding

increase in intermolecular friction causes a subsequent rise in the viscosity.

In addition, the pressure coefficients show large variations even for the same polymer. For example, some investigations show that the pressure coefficient decreases with increasing shear rate, while shear rate independent values have also been observed [19–21, 24]. The same holds for the effect of temperature. Both temperature-dependent [19, 21, 25] and independent [14, 20, 26] pressure coefficients have been reported. There is no doubt that the different measurement techniques and determination methods of pressure coefficient are the critical reasons for its great variations.

However, the existing pressure coefficient measuring procedures often require a large sample volume and a long test period. With the advancement of rheology, an increasing number of researchers are interested in small-scale testing, with the goal of enhancing data production efficiency through high-throughput experimentation (HTE) [27]. The HTE method has lately been used for viscosity measurement [28], interfacial rheology [29], material design [27], catalytic olefin polymerization [30], and other fields. Tammaro and Maffettone [31] have made a lot of cutting-edge work in characterizing polymer viscosity with custom-made microcapillary rheometers (μCR) [31–33]. Tommaro's innovative gas-pressurized multipass μCR is able to execute tests in parallel with only a few milligrams of material to reduce test time [33]. Furthermore, the ability to adjust the pressure in the exit chamber allows for high-pressurized rheological experiments, opening up a new study avenue for measuring the pressure coefficient of viscosity.

In this paper, a concise review is given about the characteristics of various measurement techniques and methods for the pressure dependence of viscosity. The accuracy and relationship of pressure coefficients determined by different methods are also discussed on the basis of published experimental data.

2. Measurement Techniques

Since Maxwell and Jung's [11] ground-breaking work on the pressure dependence of viscosity in the 1950s, numerous measurement techniques have been developed, which can be primarily divided into two categories: one involves rheometers based on drag flow, and the other involves rheometers based on pressure-driven flow [34].

2.1. Drag Flow Rheometers. Drag flows are generated by sandwiching the sample between two parallel plates and moving one plate relative to the other [20, 34]. Rotational rheometers, rotating cylinder viscometers, and sliding plate rheometers are common types of drag flow rheometers. Pressurized versions of these rheometers are designed to investigate the effect of pressure on viscosity. In 1967, Hellewege et al. [35] investigated the rheological behavior of polystyrene using a high-pressure rotational viscometer with pressure up to 150 MPa. The results demonstrated that the viscosity of polystyrene was much more reliant on pressure compared to polyolefins. Also, they found the rheological behavior of melt at low shear rates is consistent with the linear viscoelastic theory. Cogswell et al. [36] used a pressurized Couette–Hatschek rotating cylinder viscometer capable of operating at pressure ranging from atmospheric pressure to 175 MPa. They discovered that polymers with benzene rings as the main chain had larger parachor (V^*) values and that the viscosity of polymer became much more sensitive to pressure as V^* increased. However, it is laborious to load samples and time-consuming to clean the instrument due to its complex structure.

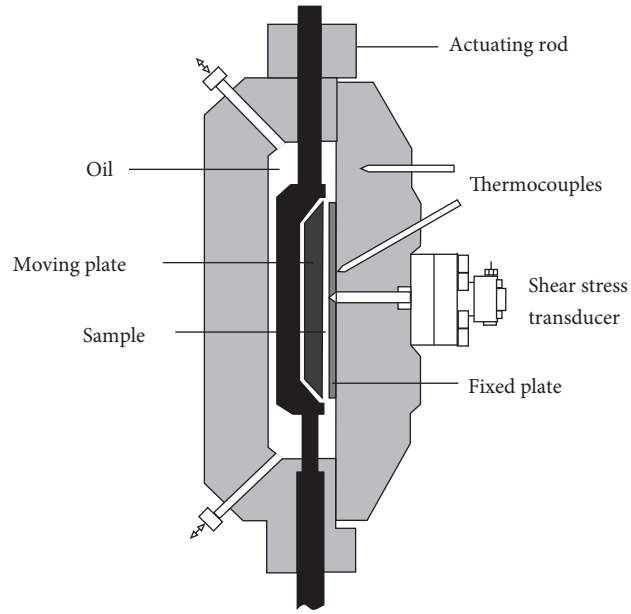

Figure 2: Schematic of a high-pressure sliding plate rheometer [20].

In 1999, Koran and Dealy [20] designed a high-pressure sliding plate rheometer capable of running at pressure up to 70 MPa and temperature up to 225°C to investigate the effect of pressure on the viscosity of polymer melts. An inert liquid that has no effect on polymers is used as the pressurized medium instead of gas. Because gas may dissolve in the melt under high pressure and thus affect the rheological properties of polymer melts [37]. In this design, the deformation of the melt is independent of pressure; thus, the pressure and the deformation rate can be controlled separately. The shear stress is measured using a shear stress transducer mounted in the middle of a fixed plate, as shown in Figure 2. The pressure is obtained using a hand pump, which can pump the inert fluid into the cavity. It is believed that the pressure of the melt is equivalent to that of the inert liquid. This high-pressure sliding plate rheometer was later used to investigate the effect of pressure on the viscosity of HDPE and PS by Park and Dealy [38] and Park et al. [39]. Since the test is often carried out under a parallel disk with a diameter of 25 mm and a gap of 1 mm, the sample volume is about 0.5 cm^3.

The advantage of a drag flow rheometer is that the generated flow is rheologically simple. In other words, the sample is subjected to uniform pressure and shear rate, making direct data processing without any corrections [10, 22]. Besides, it is beneficial to investigate the rheological properties of polymer melts at low shear rates or transient flows

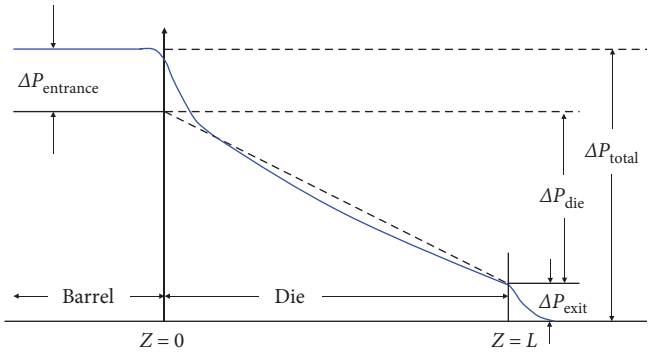

FIGURE 3: Schematic of the axial pressure profile in pressure-driven flow rheometer.

[15]. However, its applicability is restricted by the relatively small shear rate ranges and intricate mechanical configurations [10]. Therefore, in order to study the actual rheological behavior of polymers at high shear rates close to polymer processing, rheometers based on pressure-driven flow are more widely used.

2.2. Pressure-Driven Flow Rheometers. Slit rheometer and capillary rheometer are the two primary types of pressure-driven flow rheometers, which use the pressure difference between the entrance and exit of the flow geometry as the driving force. The difference between the two rheometers lies in the geometry of the die, where the slit is rectangular, and the capillary is circular. The high viscosities of polymers make it necessary to apply significant pressures to drive the flow through the die [34]. The effect of pressure on viscosity may cause nonlinear pressure distribution along the die (see Figure 3) [15, 40, 41]. Therefore, the nonlinearity of the pressure profile can be used to determine the pressure dependence of viscosity.

2.2.1. Traditional Standard Rheometers. For slit rheometer, pressure transducers can be flush mounted on the surface of a rectangular die, making a direct measurement of pressure profile. In 1983, Laun [42] designed a high-pressure slit rheometer with a pressure of up to 200 MPa by attaching the slit die to the barrel of the capillary viscometer (see Figure 4). The height and diameter of the barrel are 200 and 12 mm, respectively, which means that the volume of the loaded sample is about 23 cm^3. The impact of pressure on viscosity and entrance pressure loss can be determined by data from three pressure transducers mounted along the die and one in the barrel. Hay et al. [41] presented an approximate treatment of a fluid flowing through a slit die. They found that the pressure coefficient estimated by the curvature of the pressure profile is unreliable if viscous heating is not taken into account. Kadijk and Van Den Brule [21] measured the pressure-dependent viscosity of PP, ABS, and PS by a slit viscometer. Results showed that the pressure coefficient for ABS and PS was pressure-independent but declined with pressure for PP.

For capillary, however, the curvature of the circular die is too high to mount pressure transducers. Although the pressure profile cannot be directly measured, it can be deduced

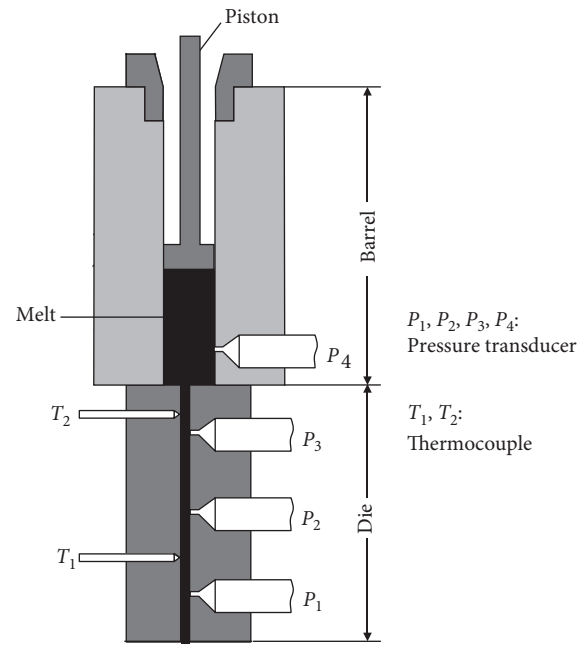

FIGURE 4: Schematic of the slit rheometer [42].

from the Bagley plot, whose curvature is used to estimate the pressure-dependent viscosity by Dudvani and Klein [43]. Nevertheless, the nonlinearity of the pressure profile can also be caused by many other factors, such as the effects of viscous heating [41, 44], wall slip [45, 46], and molecular reorientation [47, 48]. As a result, the pressure coefficient calculated from the nonlinear pressure profile is relatively reliable only for polymers with large pressure-dependent viscosities but unreliable if these effects are disregarded [10].

2.2.2. Rheometers with Counter-Piston Devices. Another direct measurement of pressure-dependent viscosity can be achieved by two simple modifications of pressure-driven rheometers. One is adding a counter piston to the downstream of the capillary die; another is adding a pressurized exit chamber. The schematic of the first modification can be seen in Figure 5(a). It first appeared in the 1950s when Maxwell and Jung [11] mounted the die between two cylinders. The plunger in each cylinder was hydraulically operated to pressurize the melt. Similarly, Westover [12] and Ito et al. [49] employed comparable devices with pressures as high as 170 and 100 MPa, respectively. In 1978, Karl [50] reduced the pressure on one piston to generate a flow through the capillary according to the back pressure principle. The maximum pressure of this device can reach 500 MPa. Mackley and Spitteler [51] used a multi-pass rheometer that could operate at steady and oscillatory modes to study the pressure-dependent rheology of LLDPE. By using servo-hydraulic control, the two pistons of the rheometer can run separately or jointly, allowing the measurement not only at a constant shear rate but also at constant shear stress. Similar to the counter-piston device, Park et al. [22] designed a counter-pressure nitrogen rheometer. As Figure 5(b) depicts, the upper gas chamber and counter-pressure reservoir are sealed and filled with nitrogen.

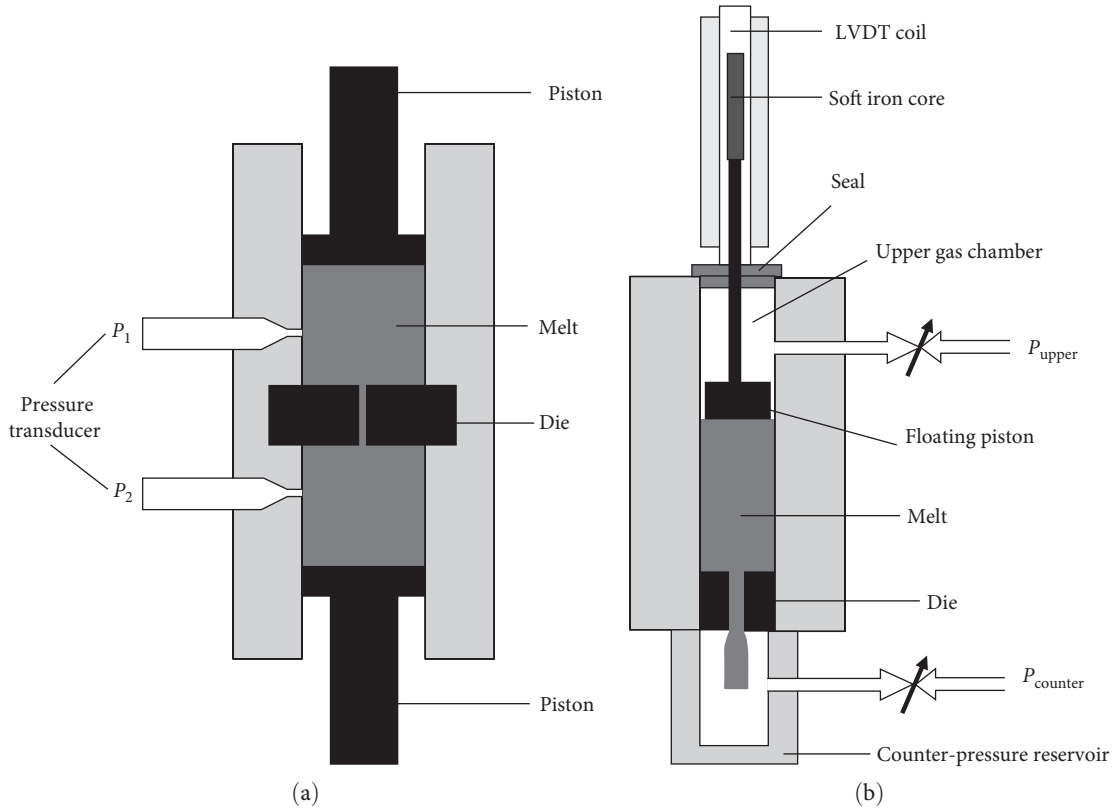

Figure 5: (a) Schematic of the rheometer with counter-piston device and (b) schematic of the rheometer with counter-pressure nitrogen device [22].

Nitrogen pressures in the chamber and reservoir can be separately regulated by precision pressure calibrators. A sample of about 12 cm^3 is required because the height of the barrel is 70 mm and the diameter is 15 mm. Apart from the capillary rheometer, a counter piston is also used in slit rheometer [21]. Son [52] reported a dual-piston rheometer with two chambers connected by a capillary or a slit. One piston moved at a constant speed while the other was kept under control at a constant pressure. However, it takes time and requires numerous attempts to loosen and tighten the adjustment screw valve in order to obtain a flow curve at a constant downstream pressure. In summary, the typical characteristic of the rheometer with a counter-piston device is independent control of melt pressure at both ends of the die, which allows constant shear stress control. Additionally, the pressure dependence of viscosity can be accurately measured in common ranges of shear rates and pressures in polymer processing. Besides, the sample consumption is small because polymer melt can flow back and forth in two chambers. However, the use of this precise pressure control device is limited due to its high cost and difficult operation and maintenance.

2.2.3. Rheometers with Pressurized Exit Chambers. For the second modification, a conical or needle valve is used to regulate the pressure at the exit of the die; thus, a hydrostatic pressure can be established in the capillary. The structure is schematically depicted in Figure 6. It comprises two pressure transducers and a valve on the downstream chamber. The overall pressure drop is changed by adjusting the valve as the piston descends at a constant speed. This method provides apparent viscosity data at a constant shear rate, and the constant shear rate pressure coefficient can be obtained by direct analysis of the data. Baker and Thomas [53] used a rheometer with a pin for adjusting the back pressure to study the effect of hydrostatic pressure on the flow properties of various polymer melts (PC, ABS, PP, HDPE) from ambient pressure to 200 MPa. Driscoll and Bogue measured the viscosity of PS at pressure as high as 124 MPa and shear rate between 1 and 100 s^{-1} by use of a back pressure-regulated capillary rheometer with a needle valve [54]. They also developed a model based on a temperature–pressure–shear-dependent time constant and a pressure-dependent elastic modulus. Later, more investigations using a piston-driven capillary rheometer with a conical valve or a needle valve were reported by Chakravorty et al. [55], Laun [56], Carreras et al. [57], Sedlacek et al. [19], Hausnerova et al. [58], Hausnerova et al. [59], Park et al. [22], Cardinaels et al. [16], Couch and Binding [14], Binding et al. [24], Raha et al. [60], Li et al. [61], and Aho and Syrjälä [10]. The main benefits of this approach are the improved accuracy and slight modifications to the standard capillary rheometers. So, the volume of the loaded sample is the same as the standard capillary rheometer. However, like the inherent drawbacks of all capillary rheometers, which are manifested in the uneven pressure and shear rate in the die as well as the

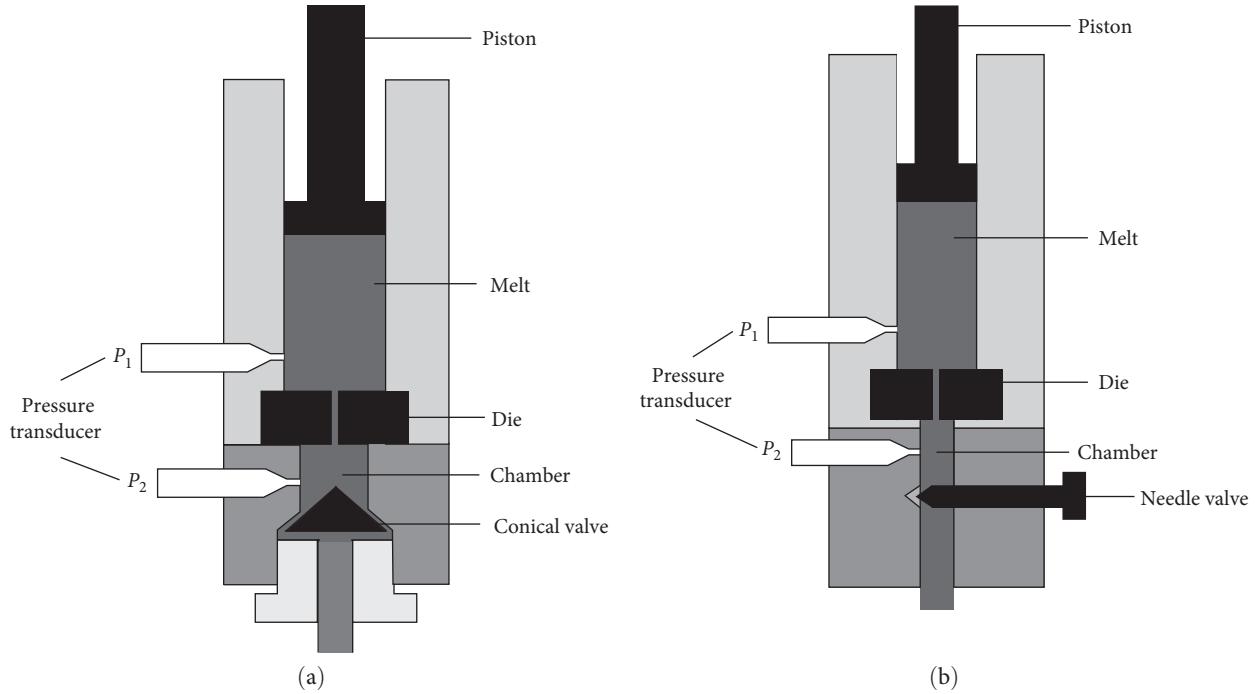

FIGURE 6: Schematic of the rheometer with a pressurized exit chamber, where the exit pressure is regulated by (a) a conical valve and (b) a needle valve.

unavoidable entrance pressure drop, varying pressure complicates data processing. Despite the shortcomings involved, this method is commonly reported in the literature because it strikes a reasonable balance between complexity and accuracy [10].

3. Determination of Pressure Coefficient

3.1. Pressure Coefficient Calculated by Nonlinear Pressure Profiles. For traditional capillary rheometry, the pressure coefficient can be inferred from Bagley plots, which are plots of pressure drop versus the ratio of length over diameter (Figure 7). Hatzikiriakos and Dealy [45] noted that the data followed straight lines at low shear rates but did not lie on straight lines at high shear rates.

The force of a microsegment fluid in the capillary is investigated. If it is assumed that there is no wall slip and the flow is fully developed steady-state laminar flow, the momentum balance equation along the capillary axis is as follows:

$$\pi R^2 dp = 2\pi R \tau_w dz, \tag{2}$$

where τ_w is the wall shear stress at pressure p and R is the radius of capillary. According to Equation (1), shear stress is exponentially dependent on pressure, which can be expressed as follows:

$$\tau_w = \eta\dot{\gamma} = \eta_{p_0}\dot{\gamma}e^{\beta p} = \tau_0 e^{\beta p}, \tag{3}$$

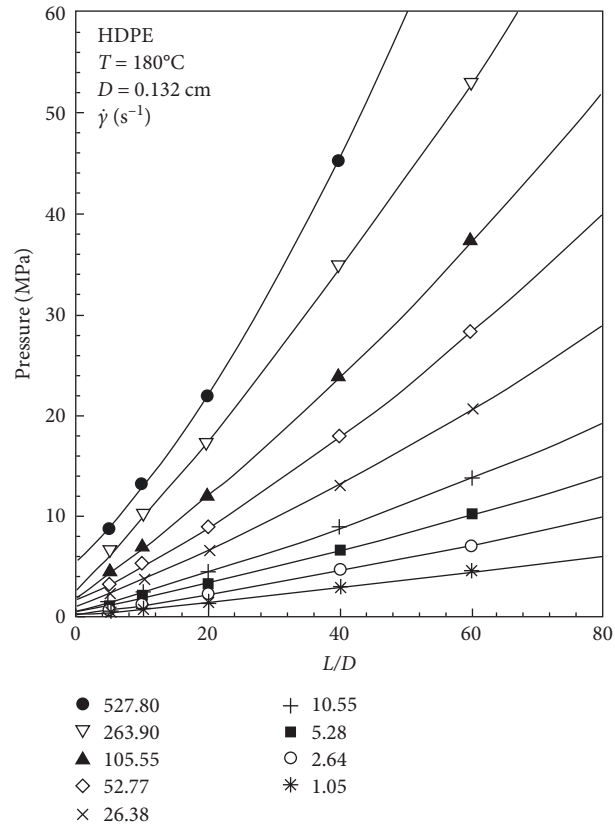

FIGURE 7: Bagley plot of HDPE (Sclair 56B/3830) [45].

where τ_0 is the wall shear stress at atmospheric pressure, and η_{p_0} is the viscosity at atmospheric pressure. According to Equations (2) and (3), one gets the following:

$$\tau_0 e^{\beta p} = \frac{\partial p}{\partial z}\frac{R}{2}. \tag{4}$$

Integral of the pressure of melt and capillary length can be expressed as follows:

$$\int_{p_{en}}^{p_{ex}} e^{-\beta p} dp = \frac{2\tau_0}{R}\int_0^L dz, \tag{5}$$

where p_{en} is the pressure at the entrance of die, p_{ex} is the pressure at the exit of die, and L is the length of die. Assuming the exit pressure is atmospheric pressure, the following equation can be obtained, that is,

$$e^{-\beta p_{en}} = 1 - 4\beta\tau_0\frac{L}{D}, \tag{6}$$

where D is the diameter of die. Then, the entrance pressure can be written as follows:

$$p_{en} = \frac{-1}{\beta}\ln\left(1 - 4\beta\tau_0\frac{L}{D}\right). \tag{7}$$

By expanding the series of Equation (7) to the quadratic term, one can obtain the following:

$$p_{en} = \frac{-1}{\beta}\left[4\beta\tau_0\frac{L}{D} + \frac{1}{2}\left(4\beta\tau_0\frac{L}{D}\right)^2\right]. \tag{8}$$

Due to the entrance pressure loss, the relation is as follows:

$$p_{en} = p_{total} - p_{loss}, \tag{9}$$

holds, where p_{total} is the total pressure drop and p_{loss} is the entrance pressure loss. Then Equation (8) can be simplified as follows:

$$p_{total} = A\left(\frac{L}{D}\right) + B\left(\frac{L}{D}\right)^2 + C. \tag{10}$$

According to Equations (8) and (10), the pressure coefficient can be then written as follows:

$$\beta = \frac{2B}{A^2}. \tag{11}$$

Therefore, the pressure coefficient can be obtained according to Equation (11) by parabolic fitting of the Bagley plot. This method has been used by Laun [42], Dudvani and Klein [43], Penwell and Porter [62], Van Puyvelde et al. [63], and Kamal and Nyun [64].

3.2. Pressure Coefficient for Zero Shear Rate Viscosity. The pressure coefficient for zero shear rate viscosity β_0 is obtained from a series of zero shear rate viscosity data of melt at different pressures, which can be expressed as follows:

$$\beta_0 = \left(\frac{d\ln\eta_0}{dp}\right)_T, \tag{12}$$

where η_0 is the viscosity at zero shear rate. The value of β_0 is relatively stable and does not vary with shear stress and shear rate. Therefore, it can be taken as the thermodynamic property of polymer melts. However, it is challenging to obtain such data in the experiment [10].

3.3. Pressure Coefficient at Constant Shear Rate. The constant shear rate pressure coefficient is defined as follows:

$$\beta_{\dot\gamma} = \left(\frac{d\ln\eta}{dp}\right)_{T,\dot\gamma}, \tag{13}$$

where p represents the hydrostatic pressure of melt. The experiment is carried out at a certain piston speed that corresponds to a constant apparent shear rate, and the exit pressure can be regulated by adjusting the valve of the counter-pressure chamber [52]. The wall shear stress is calculated from the pressure difference between the entrance and exit, taking the entrance pressure loss into account. The entrance pressure loss can be obtained directly from the orifice experiment or can be inferred from Bagley plots. The arithmetic mean of entrance and exit pressures is taken as the hydrostatic pressure of the melt in the capillary [10, 15]. As shown in Figure 8, the pressure coefficient is the slope of the straight line for the semi-log plot of viscosity and mean pressure. However, the pressure coefficient obtained by this method is not a real thermodynamic property because it varies with shear rate and temperature [14–17]. As Figure 9 shows, pressure coefficients decrease with the increasing shear rate and tend to a constant value in the power law region. Guo et al. [17] found that the relationship between pressure coefficient and temperature is similar for PET. Nevertheless, it is commonly used in literature due to its simple measurement and easy use.

3.4. Pressure Coefficient at Constant Shear Stress. The constant shear stress pressure coefficient is defined as follows:

$$\beta_\tau = \left(\frac{d\ln\eta}{dp}\right)_{T,\tau}, \tag{14}$$

where p is the hydrostatic pressure of melt. Rheometers with counter-piston devices are often used to obtain constant shear stress pressure coefficients because pressures at the entrance and exit of the die can be controlled separately. As the pressure drop ΔP remains constant, the experiment

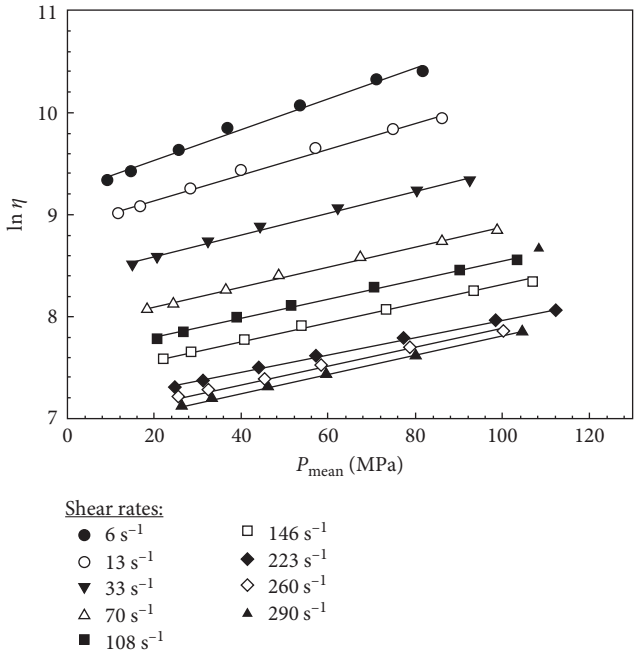

Figure 8: Determination of $\beta_{\dot{\gamma}}$ at several shear rates for PMMA ($T = 210°C$) [16].

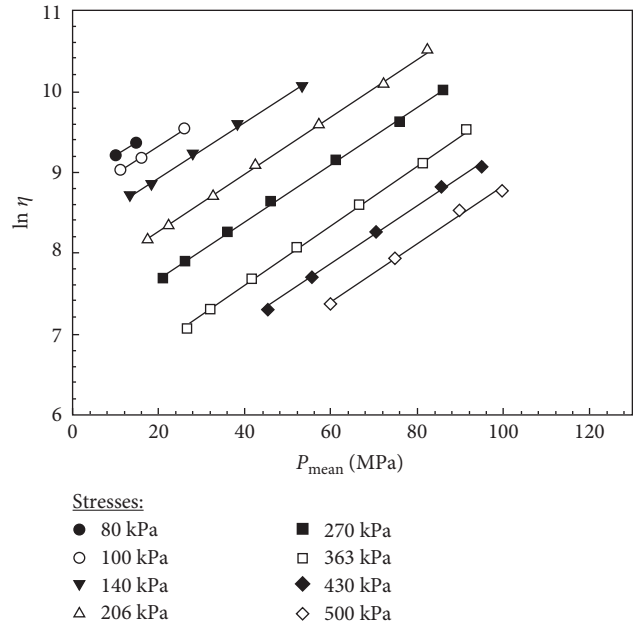

Figure 10: Determination of β_{τ} at several shear stress levels for PMMA ($T = 210°C$) [16].

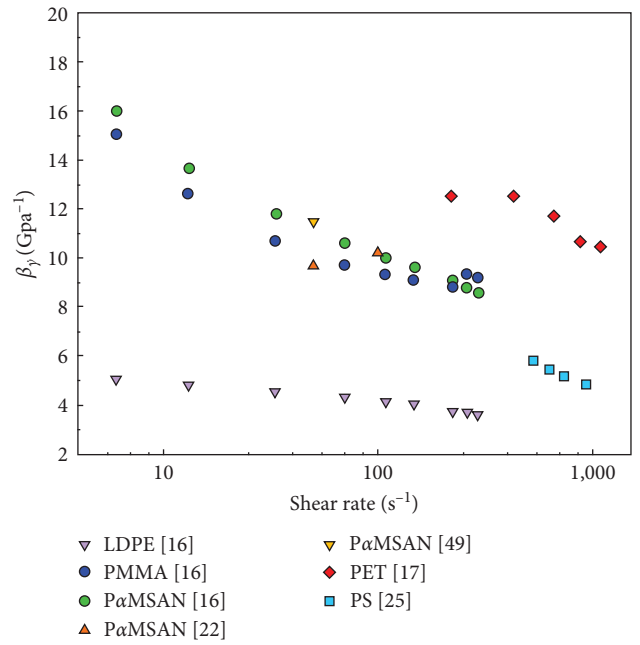

Figure 9: Pressure coefficient $\beta_{\dot{\gamma}}$ as a function of shear rate for five polymers [16, 17, 22, 25, 56].

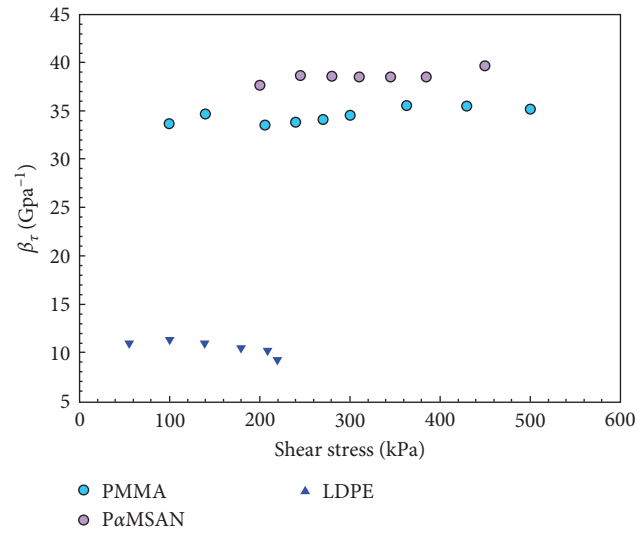

Figure 11: Pressure coefficient β_{τ} versus shear stress [16].

is conducted at constant shear stress. The pressure coefficient can be calculated from the semi-log plot of viscosity and mean pressure (see Figure 10). Cardinaels et al. [16] noticed that the straight lines under varied shear stress are practically parallel, implying the constant shear stress pressure coefficient does not dependent on shear stress. As Figure 11 illustrates, the pressure coefficients of three polymers only show a slight fluctuation with shear stress, even in the small shear rate range deviating from the power law region. Therefore, in contrast to the constant shear rate pressure coefficient, the pressure coefficient at constant shear stress can be viewed as a thermodynamic property of the polymer melt.

Nevertheless, there is a correlation between pressure coefficient at constant shear rate and constant shear stress [37], which can be expressed as follows:

$$\beta_{\dot{\gamma}} = \beta_{\tau}\left(1 + \frac{\partial \ln \eta}{\partial \ln \dot{\gamma}}\right). \quad (15)$$

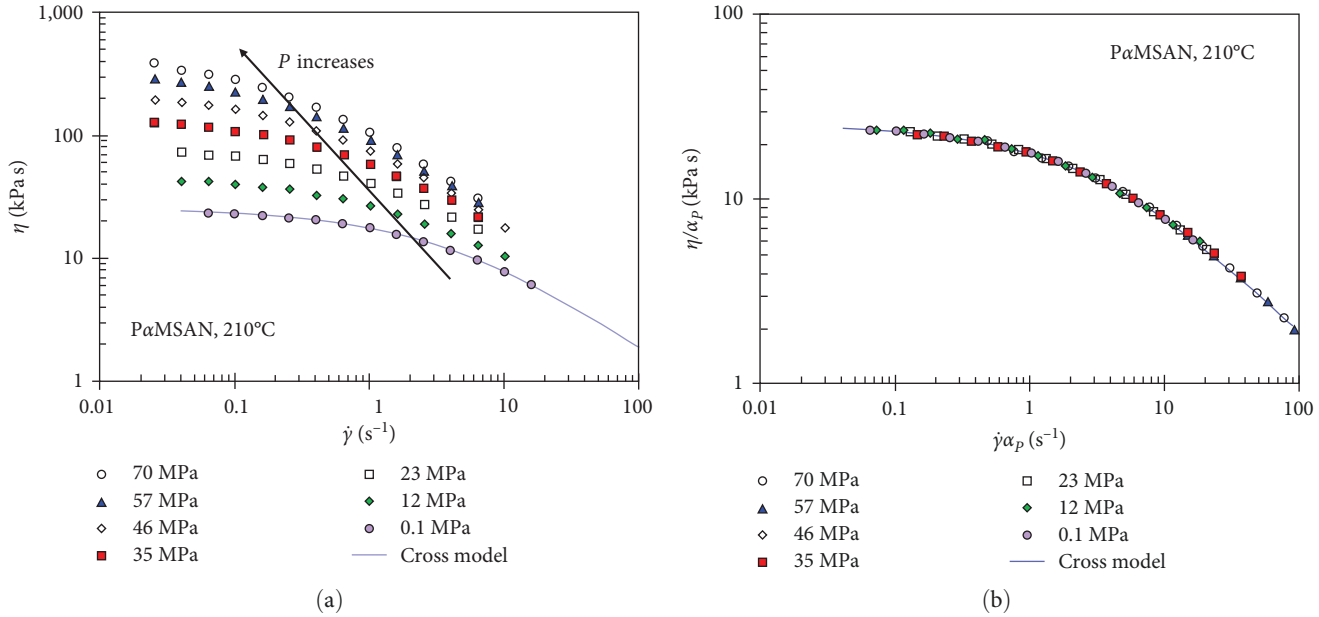

FIGURE 12: (a) Viscosity vs. shear rate at several mean pressures and (b) viscosity master curve [22].

In the Newtonian regimes, viscosity is a constant, which means $\beta_{\dot{\gamma}}$ is equal to β_τ. However, the viscosity is dependent on the shear rate in the power law region, where viscosity can be written as follows:

$$\eta = K\dot{\gamma}^{n-1}. \tag{16}$$

Therefore, Equation (15) becomes the following:

$$\beta_{\dot{\gamma}} = \beta_\tau(1 + n - 1) = n\beta_\tau. \tag{17}$$

The relationship between $\beta_{\dot{\gamma}}$ and β_τ is supported by Cardinaels et al. [16] and Park et al. [22].

3.5. Pressure Coefficient Calculated by Superposition Method. Considering the effect of temperature and pressure on viscosity, a shift factor a_{TP} is usually given by [40, 57] the following:

$$a_{\mathrm{TP}} = a_T a_P = \exp\left[\frac{E}{R'}\left(\frac{1}{T} - \frac{1}{T_{\mathrm{ref}}}\right)\right]\exp[\beta(P - P_{\mathrm{ref}})], \tag{18}$$

where R' is the gas constant, E is the activation energy, T_{ref} is the reference temperature, and P_{ref} is the reference pressure. Here, we only discuss the pressure coefficient at a single temperature, which is defined by the following:

$$\beta_P = \left(\frac{d\ln a_P}{dP}\right)_T, \tag{19}$$

where a_P is a horizontal shift factor exhibiting the response of pressure to time, which is larger than the vertical shift factor b_P [16, 22]. The process of determining the pressure coefficient by time–pressure superposition method is similar to that of determining the activation energy by time–temperature superposition method [14, 52]. As Figure 12 depicts, by multiplying the shear rate and dividing the viscosity by the shift factor a_P, flow curves of viscosity as a function of pressure can be shifted to a master curve, which can be interpreted by the following:

$$\eta(\dot{\gamma}, P) = \eta(a_P\dot{\gamma}, P_{\mathrm{ref}}). \tag{20}$$

To determine the pressure coefficient, the shift factor a_P should be obtained first. As Figure 13(a) illustrates, double logarithmic plots of viscosity and shear rate at different pressures are constructed. The viscosity curve at elevated pressure can shift to the curve at a reference pressure, and the horizontal shifting distance is ln a_P. Once the shift factors under a series of pressures are calculated, the pressure coefficient can be obtained from the slope of the semilogarithmic plot of shift factor and pressure (see Figure 13(b)).

Cardinaels et al. [16] handled data from the rheometer with a pressurized exit chamber using the superposition method. However, since the mean pressure of melt cannot be directly controlled, substantial data processing is necessary. Therefore, viscosity curves at various fixed exit pressures should be recalculated to those at mean pressures. Son [52] used a double-piston rheometer where the mean pressure can be directly controlled to avoid the drawback of extensive data handling. Park et al. [22] used the superposition method to handle data from the high-pressure sliding plate rheometer. Viscosities at different pressures fall on a master curve at low shear rates ranging from 1 to 100 s^{-1}, implying that this method applies to the transition region from Newtonian to the power law region.

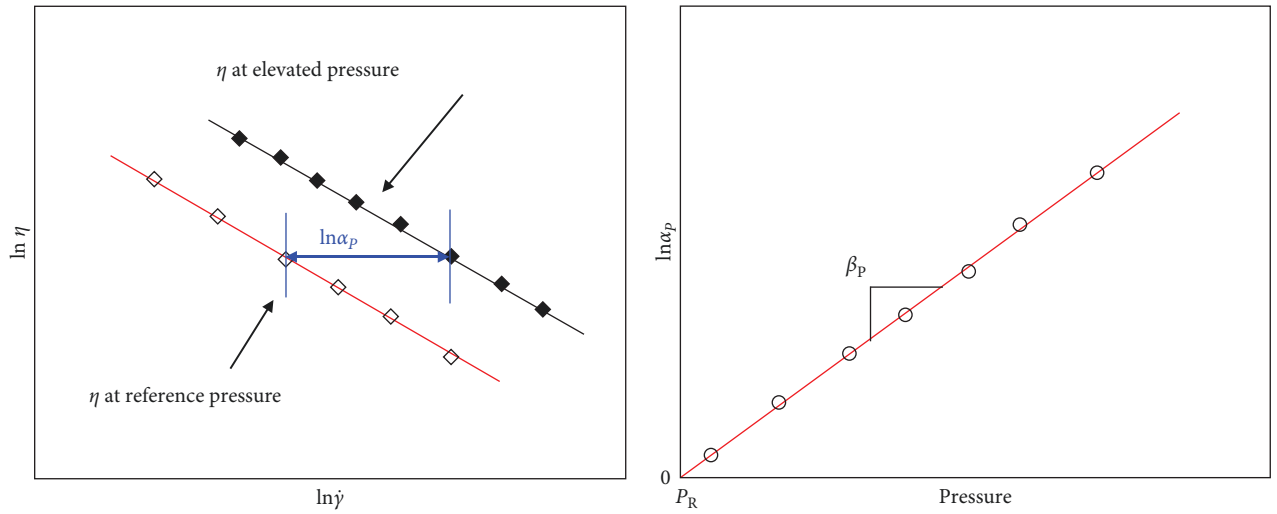

FIGURE 13: Determination of pressure coefficient by time–pressure superposition method: (a) double logarithmic plots of viscosity and shear rate; (b) semilogarithmic plot of shift factor and pressure.

3.6. Pressure Coefficient Calculated from PVT Data. Pressure, volume, and temperature are crucial parameters in polymer processing, and the dependence of polymer viscosity on pressure and temperature can be obtained by PVT data [65]. Utracki has made great efforts to study the effect of pressure on viscosity based on the free volume method [66, 67]. The pressure-dependent viscosity treated as a function of free volume fraction has been proposed [68, 69], which can be written as follows:

$$\ln \eta = a_0 + \frac{a_1}{h + a_2}, \tag{21}$$

where η is either the zero-shear viscosity or viscosity at constant shear stress, a_0 and a_1 are adjustment parameters, a_2 is an empirical value which is small and can be neglected here, h is the free volume fraction as a function of temperature and pressure: $h = h(T, P)$. Utracki [67] described the linear relationship of $1/h$ and pressure at a given temperature:

$$\frac{1}{h} = A + B\frac{P}{P^*}, \tag{22}$$

where P^* is a characteristic parameter that can be calculated by fitting the PVT data to a modified Simha–Somcynsky equation of state (S–S) [70, 71]. Therefore, according to Equations (21) and (22), the pressure coefficient can be calculated by the following:

$$\beta = \left(\frac{d \ln \eta}{dP}\right)_T = \frac{a_1 B}{P^*}. \tag{23}$$

However, the pressure coefficient obtained by PVT data is not reliable for all polymers. Sedlacek et al. [68] reported that the master curves of zero-shear viscosity versus free volume fraction for PP and PS exhibit slight deviations due to the failure of zero-shear viscosity fitting. The PVT measurements should also be carried out in a wide range of temperature and pressure to obtain viscosity as precise as possible. Besides, $\eta(T, P)$ can be predicted only in a single phase, and the treatment should change if a phase transition like crystallization happens [67].

4. Evaluation of Different Measurement Techniques and Methods for Pressure Coefficients

4.1. Evaluation of Different Measurement Techniques. For drag flow rheometers, a sample is subjected to uniform pressure and shear rate, resulting in direct data processing without any corrections. However, constrained by low shear rates, it cannot reach the high shear rates required for polymer processing. Therefore, pressure-driven rheometers that can operate at high shear rates are more widely used. Nevertheless, a sample is subjected to uneven pressure and shear rate, and the entrance pressure loss is not negligible, which requires appropriate corrections to correct pressure (Bagley correction) and shear rate (Rabinowitsch correction) [45, 72, 73].

Three main pressure-driven rheometers are often used, which can be classified as traditional standard rheometer, counter-piston rheometer, and rheometer with exit pressurized chamber. For a traditional rheometer with a slit die, pressure transducers can be mounted along the die to directly measure the pressure of melt. However, it requires a pressure transducer with high sensitivity, and the cleaning of the die is not convenient. For traditional rheometer with capillary die, however, pressure transducers cannot be mounted on the die owing to its high curvature. Considering this situation, a series of dies with different ratios of length and diameter are used to infer the pressure distribution along the die. For the counter-piston rheometer, the constant pressure drop between two ends of the die can be achieved by

Table 2: Summary of different measurement techniques.

Type of flow	Drag flow	Pressure-driven flow		
Rheometer	Rotational rheometer, rotating cylinder viscometer, sliding plate rheometer, etc.	Traditional standard rheometer	Rheometer with counter-piston device	Rheometer with pressurized exit chamber
Measurement process	Change shear rate and pressure. Then, obtain the master curve by superposition.	Obtain the nonlinear pressure profiles from pressure transducers or from the Bagley plots.	Keep pressure drop (shear stress) constant by adjusting the hydraulic system.	Keep piston speed (shear rate) constant by adjusting the valve at the exit.
Pressurizing medium	Inert liquid, gas	Piston		
Typical volume range of loaded sample	Less than 10 cm^3 (only a few cm^3)	About 20 cm^3	Between 10 and 20 cm^3	About 20 cm^3
Advantages	(1) The sample is subjected to even pressure and shear rate. (2) Data processing is straightforward without any correction.	(1) The shear rate range is wide. (2) The measurement is direct without the second pressure chamber.	(1) The shear rate range is wide. (2) It can realize accurate pressure control and constant shear stress control. (3) Sample consumption is small.	(1) The shear rate range is wide. (2) It strikes a reasonable balance between complexity and accuracy. (3) The application of this method is widespread.
Disadvantages	(1) The shear rate range is relatively small. (2) The mechanical configuration of the rheometer is intricate. (3) It is laborious to load samples and time-consuming to clean the instrument.	(1) The high curvature of the capillary makes it impossible to install the pressure sensor. (2) The pressure coefficient estimated from the nonlinear pressure profile is unreliable. (3) The pressure and shear rate are uneven, and the data processing is required.	(1) The application of this precise device is limited due to its high cost and difficult operation. (2) The pressure and shear rate are uneven, and the data processing is required.	(1) The pressure and shear rate are uneven, and the data processing is required.

Table 3: Summary of pressure coefficients calculated from different methods.

Pressure coefficient	Formula	Accuracy	Thermodynamic property	Relationship
Nonlinear pressure profiles	$\beta = \frac{2B}{A^2}$	Not reliable	No	
PVT	$\beta = \frac{a_1 B}{P^*}$			
At constant shear rate $\beta_{\dot{\gamma}}$	$\beta_{\dot{\gamma}} = \left(\frac{d\ln\eta}{dp}\right)_{T,\dot{\gamma}}$	Reliable	Yes	$\beta_{\dot{\gamma}} = n\beta_\tau$
At constant shear stress β_τ	$\beta_\tau = \left(\frac{d\ln\eta}{dp}\right)_{T,\tau}$			$\beta_\tau = \beta_P = \beta_0$
Superposition β_P	$\beta_P = \left(\frac{d\ln a_P}{dP}\right)_T$			
Zero shear rate β_0	$\beta_0 = \left(\frac{d\ln\eta_0}{dp}\right)_T$			

adjusting the hydraulic system, resulting in a direct measurement of the pressure coefficient at constant shear stress. However, the operation of a hydraulic system to keep constant mean pressure is not easy, which limits the widespread use of this device. For a rheometer with an exit pressurized chamber, only minor modification is required, and it is easy to operate. Besides, it provides a compromise between accuracy and complexity. Therefore, it is most reported in the literature. Table 2 summarizes the features of different measurement techniques.

4.2. Evaluation of Different Methods for the Pressure Coefficient. Although the method of calculating pressure coefficient by nonlinear pressure profile is simple and direct, it is not necessarily reliable. There are some inherent drawbacks of this method:

Pressure coefficients of polymers are typically of the order of 10^{-9}–$10^{-8}\,\mathrm{Pa}^{-1}$. So, the pressure profile measured is almost linear for those polymers with small pressure coefficients, especially when the sensitivity of the pressure sensor is not high. If the nonlinearity becomes dominated, the parabolic approximation is no longer accurate because it will make the pressure coefficient overestimated. Besides, many factors contribute to the nonlinearity, such as viscous heating, wall slip, and molecular reorientation. If these factors are ignored, the calculated pressure coefficients will have experimental errors. Propagation of experimental and fitting errors should also be noted [15].

The pressure coefficient for zero shear rate viscosity can be taken as the thermodynamic property of polymer. However, zero shear rate viscosities at different pressures for various polymers are not easily obtained in the experiment.

The pressure coefficient at a constant shear rate can be directly calculated by the semi-log plot of viscosity and mean pressure. However, it is not a real thermodynamic property of polymer because it varies with shear rate, pressure, and temperature. It is exciting that the pressure coefficient at constant shear rate can be related to that at constant shear stress by power index, which can be regarded as the thermodynamic property. Therefore, it is commonly used in literature due to its simple measurement and easy use.

Time–pressure superposition method is often used, too. The pressure coefficient obtained by this method is almost the same as that at constant shear stress because the superposition method is equivalent to shifting the viscosity curves at constant shear stress.

The free volume concept can also be used to explain the effects of pressure on polymer viscosity. However, the pressure coefficient obtained by PVT data is not reliable for all polymers, and it is not clear under what conditions this method is reliable. Besides, the prediction of viscosities at different temperatures and pressures is valid only for a single phase. Table 3 summarizes the pressure coefficients calculated from different methods.

5. Conclusions and Prospects

In this paper, different measurement techniques and methods of determining pressure coefficient are reviewed and compared. It can be concluded that pressure-driven rheometers are more often used to study the effect of pressure on viscosity, particularly rheometer with exit pressurized chamber because it provides a reasonable compromise between accuracy and complexity.

Besides, the accuracy of pressure coefficients obtained by the superposition method and at constant shear rate and constant shear stress are relatively high. The pressure coefficient at constant shear stress, which is equivalent to the pressure coefficient obtained by the superposition method, is regarded as the thermodynamic property of polymer melts. What is more, pressure coefficients at constant shear rate and constant shear stress can be related to each other by power index. Therefore, pressure coefficients obtained by these three methods are interconnected. Nevertheless, pressure coefficients obtained by nonlinear pressure profiles and PVT data are less reliable due to the inherent limitation of the methods.

Many researchers have put their efforts into investigating the effect of pressure on viscosity, but somehow, the experimental data is still few compared with other external factors such as stress, shear rate, and temperature. That remains to be investigated. Besides, with the development of HTE, it is possible to measure the pressure dependence of viscosity quickly by a microcapillary rheometer, using only a little quantity of polymer. Therefore, future work can focus on small-scale measurement to meet the demands of HTE, which can be further used for artificial intelligence analysis.

Data Availability

The data supporting this review are from previously reported studies and datasets, which have been cited. The processed data are available.

Conflicts of Interest

The authors declare no conflicts of interest.

Acknowledgments

This work is supported by a grant provided by the Mitsubishi Heavy Industries.

References

[1] M. van Drongelen, P. C. Roozemond, and G. W. M. Peters, "Non-isothermal crystallization of semi-crystalline polymers: the influence of cooling rate and pressure," in *Polymer Crystallization II. Advances in Polymer Science*, vol. 277, pp. 207–242, 2016.

[2] V. E. Dobrescu and C. Radovici, "Temperature dependence of melt viscosity of polymers," *Polymer Bulletin*, vol. 10, pp. 134–140, 1983.

[3] R. S. Porter and J. F. Johnson, "Temperature dependence of polymer viscosity. The influence of polymer composition," *Journal of Polymer Science Part C: Polymer Symposia*, vol. 15, no. 1, pp. 373–380, 1967.

[4] J. Aho and S. Syrjälä, "On the measurement and modeling of viscosity of polymers at low temperatures," *Polymer Testing*, vol. 27, no. 1, pp. 35–40, 2008.

[5] C. A. Hieber and H. H. Chiang, "Shear-rate-dependence modeling of polymer melt viscosity," *Polymer Engineering and Science*, vol. 32, no. 14, pp. 931–938, 1992.

[6] A. L. Kelly, T. Gough, B. R. Whiteside, and P. D. Coates, "High shear strain rate rheometry of polymer melts," *Journal of Applied Polymer Science*, vol. 114, no. 2, pp. 864–873, 2009.

[7] T. Shende, V. J. Niasar, and M. Babaei, "An empirical equation for shear viscosity of shear thickening fluids," *Journal of Molecular Liquids*, vol. 325, Article ID 115220, 2021.

[8] T. S. Chung, "Effect of a pressure-dependent viscosity on the packing stage in injection molding," *Industrial and Engineering Chemistry Research*, vol. 26, no. 1, pp. 161–163, 1987.

[9] V. Volpe and R. Pantani, "Determination of the effect of pressure on viscosity at high shear rates by using an injection molding machine," *Journal of Applied Polymer Science*, vol. 135, no. 24, Article ID 45277, 2017.

[10] J. Aho and S. Syrjälä, "Measurement of the pressure dependence of viscosity of polymer melts using a back pressure-regulated capillary rheometer," *Journal of Applied Polymer Science*, vol. 117, no. 2, pp. 1076–1084, 2010.

[11] B. Maxwell and A. Jung, "Hydrostatic pressure effect on polymer melt viscosity," *Modern Plastics*, vol. 35, no. 3, pp. 174–182, 1957.

[12] R. F. Westover, "Effect of hydrostatic pressure on polyethylene melt rheology," *Polymer Engineering and Science*, vol. 1, no. 1, pp. 14–20, 1961.

[13] C. Barus, "Note on the dependence of viscosity on pressure and temperature," in *Proceedings of the American Academy of Arts and Sciences*, vol. 27, pp. 13–18, 1891.

[14] M. A. Couch and D. M. Binding, "High pressure capillary rheometry of polymeric fluids," *Polymer*, vol. 41, no. 16, pp. 6323–6334, 2000.

[15] A. Goubert, J. Vermant, P. Moldenaers, A. Göttfert, and B. Ernst, "Comparison of measurement techniques for evaluating the pressure dependence of the viscosity," *Applied Rheology*, vol. 11, no. 1, pp. 26–37, 2001.

[16] R. Cardinaels, P. Van Puyvelde, and P. Moldenaers, "Evaluation and comparison of routes to obtain pressure coefficients from high-pressure capillary rheometry data," *Rheologica Acta*, vol. 46, pp. 495–505, 2007.

[17] Z.-G. Guo, X. Li, J. Li, B. Zhang, and B.-W. Cheng, "Influence of reverse pressure on the shear viscosity of hydrophilic poly (ethylene terephthalate) melt," *Chinese Journal of Polymer Science*, vol. 32, pp. 923–930, 2014.

[18] H. M. Laun, "Pressure dependent viscosity and dissipative heating in capillary rheometry of polymer melts," *Rheologica Acta*, vol. 42, pp. 295–308, 2003.

[19] T. Sedlacek, M. Zatloukal, P. Filip, A. Boldizar, and P. Saha, "On the effect of pressure on the shear and elongational viscosities of polymer melts," *Polymer Engineering and Science*, vol. 44, no. 7, pp. 1328–1337, 2004.

[20] F. Koran and J. M. Dealy, "A high pressure sliding plate rheometer for polymer melts," *Journal of Rheology*, vol. 43, no. 5, pp. 1279–1290, 1999.

[21] S. E. Kadijk and B. H. A. A. Van Den Brule, "On the pressure dependency of the viscosity of molten polymers," *Polymer Engineering and Science*, vol. 34, no. 20, pp. 1535–1546, 1994.

[22] H. E. Park, S. T. Lim, H. M. Laun, and J. M. Dealy, "Measurement of pressure coefficient of melt viscosity: drag flow versus capillary flow," *Rheologica Acta*, vol. 47, pp. 1023–1038, 2008.

[23] A. L. Isayev, *Injection and Compressing Molding Fundamentals*, CRC Press, New York, USA, 1987.

[24] D. M. Binding, M. A. Couch, and K. Walters, "The pressure dependence of the shear and elongational properties of polymer melts," *Journal of Non-Newtonian Fluid Mechanics*, vol. 79, no. 2-3, pp. 137–155, 1998.

[25] J.-Z. Liang, "Pressure effect of viscosity for polymer fluids in die flow," *Polymer*, vol. 42, no. 8, pp. 3709–3712, 2001.

[26] R. Pantani and A. Sorrentino, "Pressure effect on viscosity for atactic and syndiotactic polystyrene," *Polymer Bulletin*, vol. 54, pp. 365–376, 2005.

[27] J. N. Kumar, Q. X. Li, and J. Ye, "Challenges and opportunities of polymer design with machine learning and high throughput experimentation," *MRS Communications*, vol. 9, pp. 537–544, 2019.

[28] D. Moon and K. B. Migler, "Measurement of dynamic capillary pressure and viscosity via the multi-sample micro-slit rheometer," *Chemical Engineering Science*, vol. 64, no. 22, pp. 4537–4542, 2009.

[29] J. D. Martin, J. N. Marhefka, K. B. Migler, and S. D. Hudson, "Interfacial rheology through microfluidics," *Advanced Materials*, vol. 23, no. 3, pp. 426–432, 2011.

[30] A. Vittoria, G. Urciuoli, S. Costanzo et al., "Extending the high-throughput experimentation (HTE) approach to catalytic olefin polymerizations: from catalysts to materials," *Macromolecules*, vol. 55, no. 12, pp. 5017–5026, 2022.

[31] D. Tammaro and P. L. Maffettone, "A versatile and customizable low-cost printed multipass microrheometer for high-throughput polymers rheological experimentation," *Physics of Fluids*, vol. 35, Article ID 063116, 2023.

[32] D. Tammaro, "Rheological characterization of complex fluids through a table–top 3D printer," *Rheological Acta*, vol. 61, pp. 761–772, 2022.
[33] D. Tammaro, G. D'Avino, S. Costanzo, E. D. Maio, N. Grizzuti, and P. L. Maffettone, "A microcapillary rheometer for microliter sized polymer characterization," *Polymer Testing*, vol. 102, Article ID 107332, 2021.
[34] G. Hay, M. E. Mackay, S. A. McGlashan, and Y. Park, "Comparison of shear stress and wall slip measurement techniques on a linear low density polyethylene," *Journal of Non-Newtonian Fluid Mechanics*, vol. 92, no. 2-3, pp. 187–201, 2000.
[35] K. H. Hellwege, W. Knappe, F. Paul, and V. Semjonow, "Druckabhängigkeit der viskosität einiger polystyrolschmelzen," *Rheologica Acta*, vol. 6, pp. 165–170, 1967.
[36] F. N. Cogswell and J. C. McGowan, "The effects of pressure and temperature upon the viscosities of liquids with special reference to polymeric liquids," *British Polymer Journal*, vol. 4, no. 3, pp. 183–198, 1972.
[37] H. Münstedt, "Influence of hydrostatic pressure on rheological properties of polymer melts—a review," *Journal of Rheology*, vol. 64, no. 3, pp. 751–774, 2020.
[38] H. E. Park and J. M. Dealy, "Effects of pressure and supercritical fluids on the viscosity of polyethylene," *Macromolecules*, vol. 39, no. 16, pp. 5438–5452, 2006.
[39] H. E. Park, J. Dealy, and H. Münstedt, "Influence of long-chain branching on time-pressure and time-temperature shift factors for polystyrene and polyethylene," *Rheologica Acta*, vol. 46, pp. 153–159, 2006.
[40] E. Mitsoulis and S. G. Hatzikiriakos, "Rheological properties related to extrusion of polyolefins," *Polymers*, vol. 13, no. 4, Article ID 489, 2021.
[41] G. Hay, M. E. Mackay, K. M. Awati, and Y. Park, "Pressure and temperature effects in slit rheometry," *Journal of Rheology*, vol. 43, no. 5, pp. 1099–1116, 1999.
[42] H. M. Laun, "Polymer melt rheology with a slit die," *Rheologica Acta*, vol. 22, pp. 171–185, 1983.
[43] I. J. Duvdevani and I. Klein, "Analysis of polymer melt flow in capillaries including pressure effects," *SPE Journal*, vol. 23, no. 12, pp. 41–45, 1967.
[44] R. C. Warren, "Viscous heating," in *Rheological Measurement*, A. Collyer and D. W. Clegg, Eds., pp. 119–149, Springer, Dordrecht, Netherlands, 1998.
[45] S. G. Hatzikiriakos and J. M. Dealy, "Wall slip of molten high density polyethylenes. II. Capillary rheometer studies," *Journal of Rheology*, vol. 36, no. 4, pp. 703–741, 1992.
[46] J. L. Leblanc, "Wall slip and compressibility like effects in capillary rheometer tests on complex polymer systems," *Plastics, Rubber and Composites*, vol. 30, no. 6, pp. 282–293, 2013.
[47] P. Moldenaers, J. Vermant, J. Mewis, and I. Heynderickx, "Origin of nonlinearities in the Bagley plots of thermotropic copolyesters," *Journal of Rheology*, vol. 40, no. 2, pp. 203–219, 1996.
[48] H. C. Langelaan, A. D. Gotsis, and A. Posthuma de Boer, "On the linearity of the pressure drop during flow of thermotropic LCPs in slits and capillaries," *Journal of Rheology*, vol. 38, no. 5, pp. 1353–1368, 1994.
[49] K. Ito, M. Tsutsui, M. Kasajima, and T. Ojima, "Capillary flow of polymer melts under hydrostatic pressure," *Applied Polymer Symposia*, vol. 20, pp. 109–121, 1973.
[50] V. H. Karl, "Über die druckabhängigkeit der viskoelastischen und physikalisch-chemischen eigenschaften von polymeren, 8. Die viskosität von polyethylen bis 5000 bar," *Die Angewandte Makromolekulare Chemie*, vol. 79, no. 1, pp. 11–19, 1979.
[51] M. R. Mackley and P. H. J. Spitteler, "Experimental observations on the pressure-dependent polymer melt rheology of linear low density polyethylene, using a multi-pass rheometer," *Rheologica Acta*, vol. 35, pp. 202–209, 1996.
[52] Y. Son, "Measurement of pressure dependence on the shear viscosity of polymer melts," *Journal of Polymer Research*, vol. 16, pp. 667–671, 2009.
[53] F. S. Baker and M. Thomas, "The effect of hydrostatic pressure on the flow properties of various polymers," *Makromolekulare Chemie. Macromolecular Symposia*, vol. 68, no. 1, pp. 13–24, 1993.
[54] P. D. Driscoll and D. C. Bogue, "Pressure effects in polymer melt rheology," *Journal of Applied Polymer Science*, vol. 39, no. 8, pp. 1755–1768, 1990.
[55] S. Chakravorty, M. Rides, C. Allen, and C. S. Brown, "Polymer melt viscosity increases under pressure—a simple new measurement method," *Plastics Rubber and Composites Processing and Applications*, vol. 25, no. 5, pp. 260-261, 1996.
[56] H. M. Laun, "Capillary rheometry for polymer melts revisited," *Rheologica Acta*, vol. 43, pp. 509–528, 2004.
[57] E. S. Carreras, N. E. Kissi, J.-M. Piau, F. Toussaint, and S. Nigen, "Pressure effects on viscosity and flow stability of polyethylene melts during extrusion," *Rheologica Acta*, vol. 45, pp. 209–222, 2006.
[58] B. Hausnerova, T. Sedlacek, R. Slezak, and P. Saha, "Pressure-dependent viscosity of powder injection moulding compounds," *Rheologica Acta*, vol. 45, pp. 290–296, 2006.
[59] B. Hausnerova, T. Sedlacek, and P. Vltavska, "Pressure-affected flow properties of powder injection moulding compounds," *Powder Technology*, vol. 194, no. 3, pp. 192–196, 2009.
[60] S. Raha, H. Sharma, M. Senthilmurugan, S. Bandyopadhyay, and P. Mukhopadhyay, "Determination of the pressure dependence of polymer melt viscosity using a combination of oscillatory and capillary rheometer," *Polymer Engineering and Science*, vol. 60, no. 3, pp. 517–523, 2019.
[61] C. Li, F. Jiang, L. Wu, X. Yuan, and X. Li, "Determination of the pressure dependence of the shear viscosity of polymer melts using a capillary rheometer with an attached counter pressure chamber," *Journal of Macromolecular Science, Part B: Physics*, vol. 54, no. 9, pp. 1029–1041, 2015.
[62] R. C. Penwell and R. S. Porter, "Effect of pressure in capillary flow of polystyrene," *Journal of Polymer Science Part A-2: Polymer Physics*, vol. 9, no. 3, pp. 463–482, 1971.
[63] P. Van Puyvelde, A. Vananroye, A.-S. Hanot, M. Dees, M. Mangnus, and N. Hermans, "On the pressure dependency of the Bagley correction," *International Polymer Processing*, vol. 28, no. 5, pp. 558–564, 2013.
[64] M. R. Kamal and H. Nyun, "The effect of pressure on the shear viscosity of polymer melts," *Transactions of the Society of Rheology*, vol. 17, no. 2, pp. 271–285, 1973.
[65] E. Rojo, M. Fernández, M. E. Muñoz, and A. Santamaría, "Relation between PVT measurements and linear viscosity in isotactic and syndiotactic polypropylenes," *Polymer*, vol. 47, no. 23, pp. 7853–7858, 2006.
[66] L. A. Utracki, "Pressure dependence of Newtonian viscosity," *Polymer Engineering and Science*, vol. 23, no. 8, pp. 446–451, 1983.
[67] L. A. Utracki, "A method of computation of the pressure effect on melt viscosity," *Polymer Engineering and Science*, vol. 25, no. 11, pp. 655–668, 1985.

[68] T. Sedlacek, R. Cermak, B. Hausnerova, M. Zatloukal, A. Boldizar, and P. Saha, "On PVT and rheological measurements of polymer melts," *International Polymer Processing*, vol. 20, no. 3, pp. 286–295, 2005.
[69] L. A. Utracki and T. Sedlacek, "Free volume dependence of polymer viscosity," *Rheologica Acta*, vol. 46, pp. 479–494, 2007.
[70] R. Simha and T. Somcynsky, "On the statistical thermodynamics of spherical and chain molecule fluids," *Macromolecules*, vol. 2, no. 4, pp. 342–350, 1969.
[71] R. Simha, "Polymer and oligomer melts: thermodynamics, correlations, and lattice-hole theory," *Polymer Engineering and Science*, vol. 36, no. 12, pp. 1567–1573, 1996.
[72] Z. Y. Wang, S. C. Joshi, Y. C. Lam, and X. Chen, "End pressure corrections in capillary rheometry of concentrated suspensions," *Journal of Applied Polymer Science*, vol. 114, no. 3, pp. 1738–1745, 2009.
[73] B. Rabinowitsch, "Über die viskosität und elastizität von solen," *Zeitschrift für Physikalische Chemie*, no. 1, pp. 1–26, 1929.